Six-field two-fluid simulations on edge localized modes with BOUT++

BOUT++
Boundary Plasma Turbulence Code

T. Y. Xia[1,2], X. Q. Xu[2], B. Gui[1,2], Z. X. Liu[1,2], P. W. Xi[1,3], and S. C. Liu[1,2]

[1]Institute of Plasma Physics, Chinese Academy of Sciences, Hefei, China.
[2]Lawrence Livermore National Laboratory, Livermore, CA 94550, USA
[3]Peking University, Beijing, China

54th Annual Meeting of the APS Division of Plasma Physics,

Oct 31, 2012, Providence, Rhode Island, USA

This work was performed under the auspices of the U.S. DoE by LLNL under Contract DE-AC52-07NA27344 and is supported by the China NSF under Contract No.10721505, the National Magnetic Confinement Fusion Science Program of China under Contracts No. 2011GB107001.LLNL-PRES-597952

Principal Results

(1) **Series of 2-fluid models are developed in BOUT++ to simulate ELM crash.**

(2) **Fundamental model: 3-field 2-fluid model is a good enough model for P-B instability and ELM crashes.**

(3) **6-field model is developed and it is well consistent with 3-field model. This model is a useful tool to study particle and energy transport.**

(4) **High-n P-B mode is strongly stabilized at low density by diamagnetic drifts at low temperature.**

(5) **Thermal conductivities can sufficiently prevent the perturbations to penetrate into the inner boundary.**

(6) **Thermal conductivities can sufficiently suppress and narrow the particle transport at peak gradient region.**

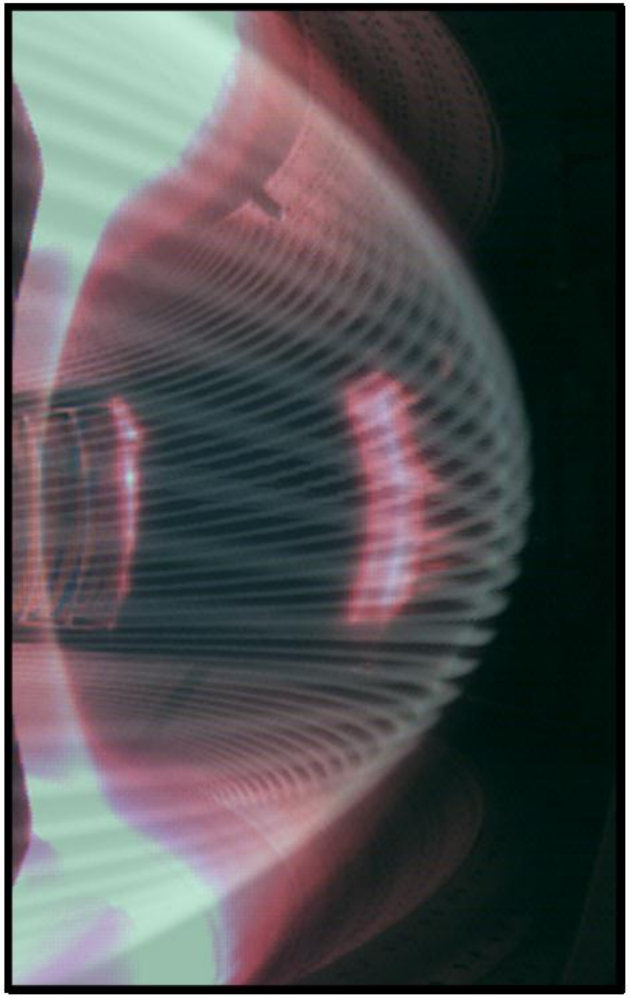

*Figure by Z. X. Liu, W.H. Meyer and J. H. Yang

BOUT++ code for modeling tokamak edge ELMs and turbulence*

- **Framework for writing fluid / plasma simulations in complex tokamak geometry**
  - **Proximity of open+closed flux surface**
  - **Presence of X-point**
- **Well benchmarked with ELITE, GATO and other codes**

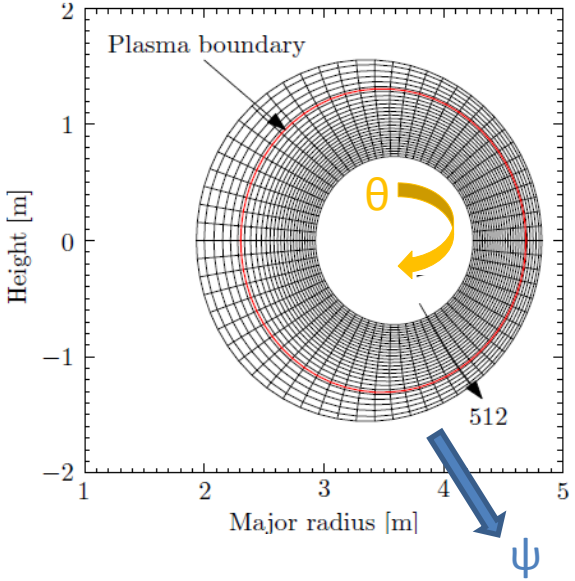

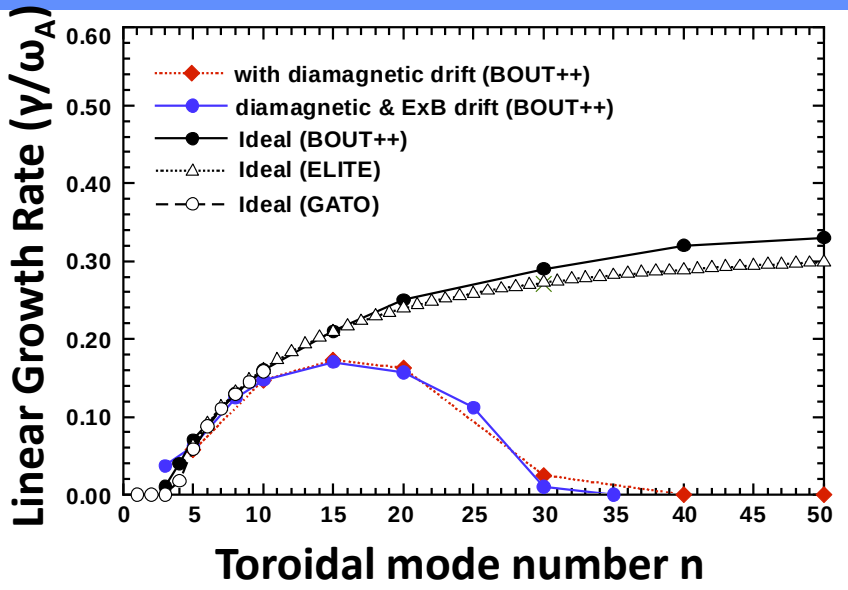

X.Q. Xu, B.D. Dudson, P.B. Snyder, M.V. Umansky, H.R.Wilson and T. Casper, Nucl. Fusion 51 (2011) 103040

Simulations are based on the shifted circular cross-section toroidal equilibria (cbm18_dan8 and cbm18_den6) generated by the TOQ code*. The equilibrium pressure is the same for all cases.

- ➢JET-like aspect ratio
- ➢Highly unstable to ballooning modes ($\gamma \sim 0.2\omega_A$)
- ➢Widely used by NIMROD, M3D, M3D-C1

** X.Q. Xu and R.H. Cohen, Contrib. Plasma Phys. 38, 158 (1998)*

- Umansky, Xu, Dudson, et al., , Comp. Phys. Comm. V. *180 , 887-903 (2008).*
- Dudson, Umansky, Xu et al., Comp. Phys. Comm. V.180 (2009) 1467.

Multi-field two-fluid model in BOUT++

- Three-field (ϖ, P, $A_{||}$): peeling-ballooning model.
- Four-field (ϖ, P, $A_{||}$, $V_{||}$): include sound waves.
- Five-field (ϖ, n_i, T_i, T_e, $A_{||}$): parallel thermal conductivities
- Six-field (ϖ, n_i, T_i, T_e, $A_{||}$, $V_{||}$): combine all the models together, based on Braginskii equations, the density, momentum and energy of ions and electrons are described in drift ordering[1].

[1]X. Q. Xu et al., Commun. Comput. Phys. **4**, 949 (2008).

ELM crash in BOUT++ simulations

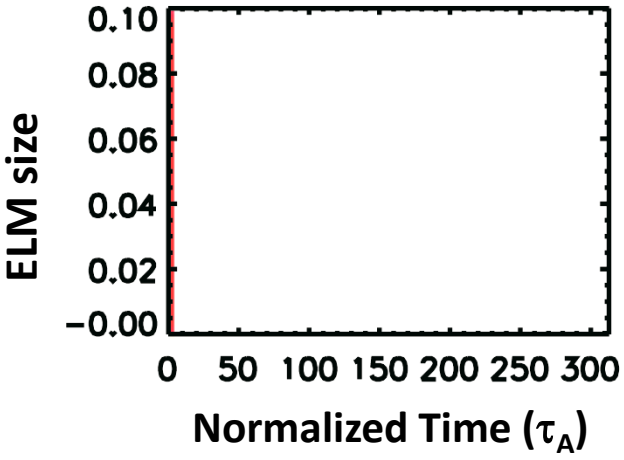

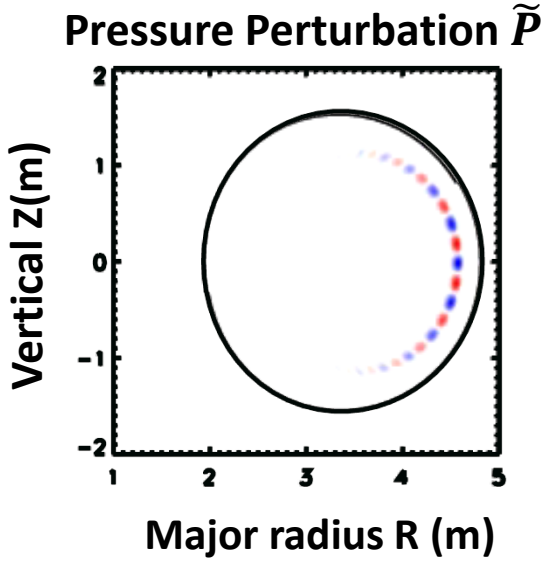

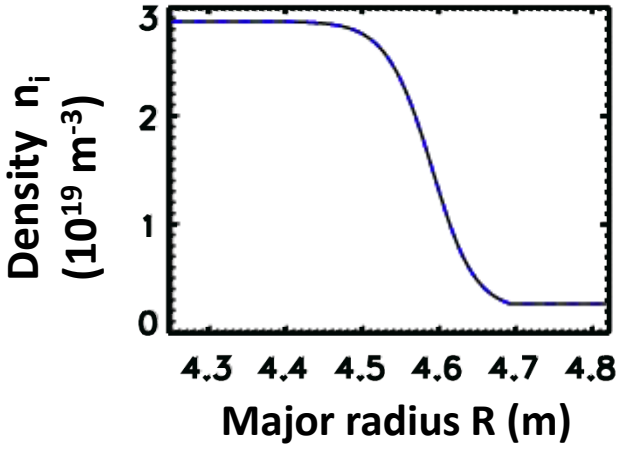

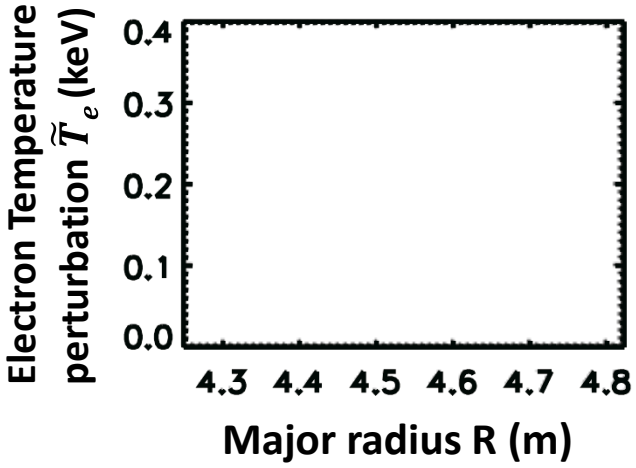

Five-field model: low density leads to larger stabilizing effects by diamagnetic drifts, and density gradient drives larger ELM size

3-field:

$$\frac{\partial P}{\partial t} + \mathbf{V}_E \cdot \nabla P = 0 \quad (previous\ model)$$

5-field

$$\frac{\partial n_i}{\partial t} + \mathbf{V}_E \cdot \nabla n_i = 0,$$

$$\frac{\partial T_j}{\partial t} + \mathbf{V}_E \cdot \nabla T_j = \nabla_\parallel \left(\kappa_{\parallel j} \nabla_\parallel T_j\right)$$

$$\varpi = n_{i0} \frac{m_i}{B_0} \left[\nabla_\perp^2 \phi + \frac{1}{n_{i0}} \nabla_\perp \phi \cdot \nabla_\perp n_{i0} + \frac{1}{n_{i0} Z_i e} \nabla_\perp^2 p_i\right]$$

With fixed pressure profile, ion density gradient leads to larger ELM size.

Density quantity affects linear growth rate through $\omega_* \propto 1/n_i$

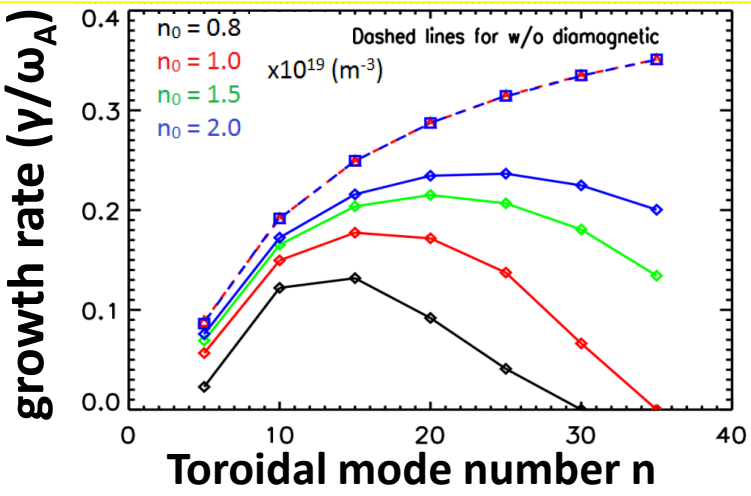

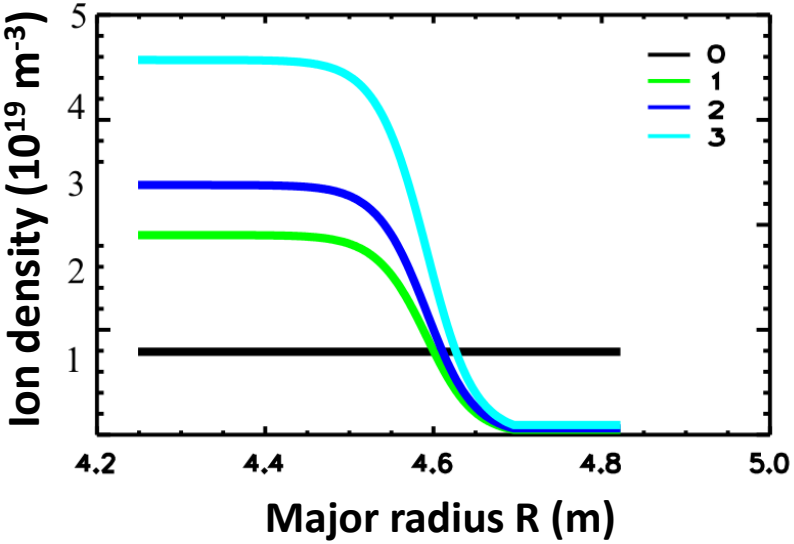

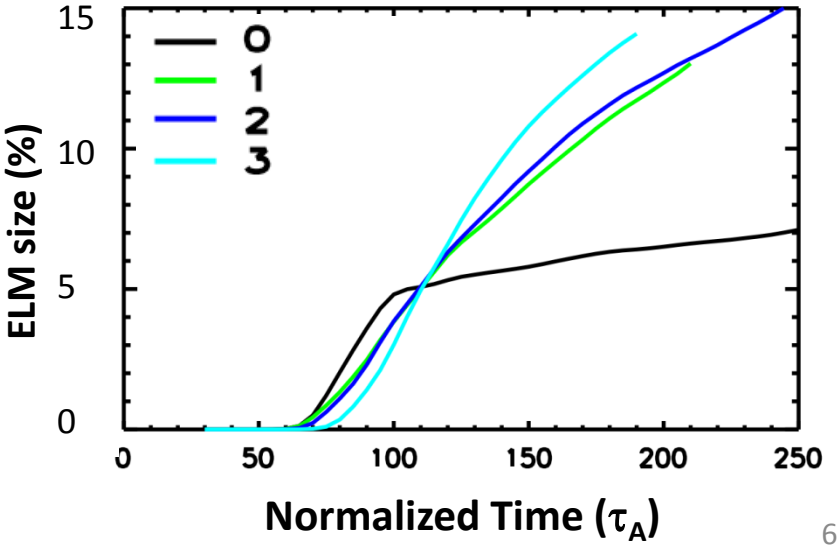

6-field 2-fluid model is derived directly from Braginskii equations and includes complete physics

$$\frac{\partial}{\partial t}\varpi = -\left(\frac{1}{B_0}\boldsymbol{b}\times\boldsymbol{\nabla}_\perp\Phi + V_{\|e}\boldsymbol{b}\right)\cdot\boldsymbol{\nabla}\varpi + B^2\nabla_\|\left(\frac{J_\|}{B}\right) + 2\boldsymbol{b}\times\boldsymbol{\kappa}\cdot\boldsymbol{\nabla}P$$

$$-\frac{1}{2\Omega_i}\left[\frac{1}{B}\boldsymbol{b}_0\times\boldsymbol{\nabla}P_i\cdot\boldsymbol{\nabla}\left(\nabla_\perp^2\Phi\right) - Z_ieB\boldsymbol{b}\times\boldsymbol{\nabla}n_i\cdot\boldsymbol{\nabla}\left(\frac{\nabla\Phi}{B}\right)^2 + Z_ieB\boldsymbol{b}\times\boldsymbol{\nabla}n_i\cdot\boldsymbol{\nabla}\left(\frac{\nabla_\|\Phi}{B}\right)^2\right]$$
$$+\frac{1}{2\Omega_i}\left[\frac{1}{B}\boldsymbol{b}_0\times\boldsymbol{\nabla}\Phi\cdot\boldsymbol{\nabla}\left(\nabla_\perp^2P_i\right) - \nabla_\perp^2\left(\frac{1}{B}\boldsymbol{b}_0\times\boldsymbol{\nabla}\Phi\cdot\boldsymbol{\nabla}P_i\right)\right],$$

$$\frac{\partial}{\partial t}n_i = -\left(\frac{1}{B_0}\boldsymbol{b}\times\boldsymbol{\nabla}_\perp\Phi + V_{\|i}\boldsymbol{b}\right)\cdot\nabla n_i - \frac{2n_i}{B}\boldsymbol{b}\times\boldsymbol{\kappa}\cdot\boldsymbol{\nabla}_\perp\Phi - \frac{2}{Z_ieB}\boldsymbol{b}\times\boldsymbol{\kappa}\cdot\boldsymbol{\nabla}_\perp P - n_iB\nabla_\|\left(\frac{V_{\|i}}{B}\right)$$

$$\frac{\partial}{\partial t}A_\| = -\nabla_\|\phi - \eta J_{\|1} + \frac{1}{en_e}\nabla_\|P_e + \frac{0.71k_B}{e}\nabla_\|T_e$$

$$\frac{\partial}{\partial t}V_{\|i} = -\left(\frac{1}{B_0}\boldsymbol{b}\times\boldsymbol{\nabla}_\perp\Phi + V_{\|i}\boldsymbol{b}\right)\cdot\boldsymbol{\nabla}V_{\|i} - \frac{1}{m_in_i}\boldsymbol{b}\cdot\boldsymbol{\nabla}P,$$

$$\frac{\partial}{\partial t}T_i = -\left(\frac{1}{B_0}\boldsymbol{b}\times\boldsymbol{\nabla}_\perp\Phi + V_{\|i}\boldsymbol{b}\right)\cdot\boldsymbol{\nabla}T_i - \frac{2}{3}T_i\left[\left(\frac{2}{B}\boldsymbol{b}\times\boldsymbol{\kappa}\right)\cdot\left(\boldsymbol{\nabla}\Phi + \frac{1}{Z_ien_i}\boldsymbol{\nabla}P_i + \frac{5}{2}\frac{k_B}{Z_ie}\boldsymbol{\nabla}T_i\right) + B\nabla_\|\left(\frac{V_{\|i}}{B}\right)\right]$$
$$+\frac{2}{3n_ik_B}\nabla_\|\left(\kappa_{\|i}\nabla_\|T_i\right) + \frac{2}{3n_ik_B}\nabla_\perp\left(\kappa_{\perp i}\nabla_\perp T_i\right) + \frac{2m_e}{m_i}\frac{Z_i}{\tau_e}\left(T_e - T_i\right)$$

$$\frac{\partial}{\partial t}T_e = -\left(\frac{1}{B_0}\boldsymbol{b}\times\boldsymbol{\nabla}_\perp\Phi + V_{\|e}\boldsymbol{b}\right)\cdot\boldsymbol{\nabla}T_e - \frac{2}{3}T_e\left[\left(\frac{2}{B}\boldsymbol{b}\times\boldsymbol{\kappa}\right)\cdot\left(\boldsymbol{\nabla}\Phi - \frac{1}{en_e}\boldsymbol{\nabla}P_e - \frac{5}{2}\frac{k_B}{e}\boldsymbol{\nabla}T_e\right) + B\nabla_\|\left(\frac{V_{\|e}}{B}\right)\right]$$
$$-0.71\frac{2T_e}{3en_e}B\nabla_\|\left(\frac{J_\|}{B}\right) + \frac{2}{3n_ek_B}\nabla_\|\left(\kappa_{\|e}\nabla_\|T_e\right) + \frac{2}{3n_ek_B}\nabla_\|\left(\kappa_{\perp e}\nabla_\perp T_e\right)$$
$$-\frac{2m_e}{m_i}\frac{1}{\tau_e}\left(T_e - T_i\right) + \frac{2}{3n_ek_B}\eta_\|J_\|^2$$

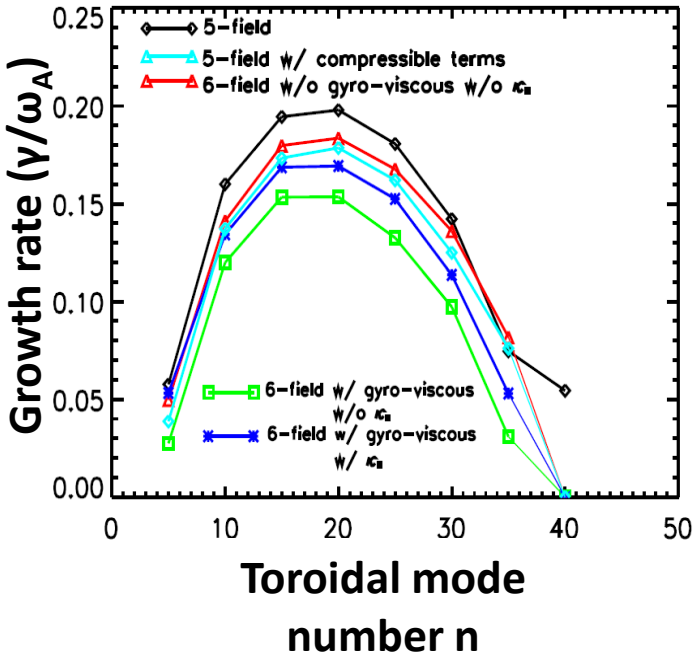

Compressible terms

Parallel velocity terms

Electron Hall

Thermal force

Gyro-viscosity

Energy exchange

Energy flux

Thermal conductivities prevent energy transport to penetrate to inner boundary

- Thermal conductivities with flux limited expressions suppress the increase of ELM

$$\kappa_{\|i} = 3.9\frac{v_{th,i}^2}{\nu_i} \quad \kappa_{\|e} = 3.2\frac{v_{th,e}^2}{\nu_e} \quad \kappa_{fl,j} = v_{th,j} q_{95} R_0$$

Flux limited expression:

$$\kappa_{\|j}^{e} = \left(\frac{1}{\kappa_{\|j}} + \frac{1}{\kappa_{fl,j}}\right)^{-1}$$

Electron temperature is most sensitive to $\kappa_{||}$.

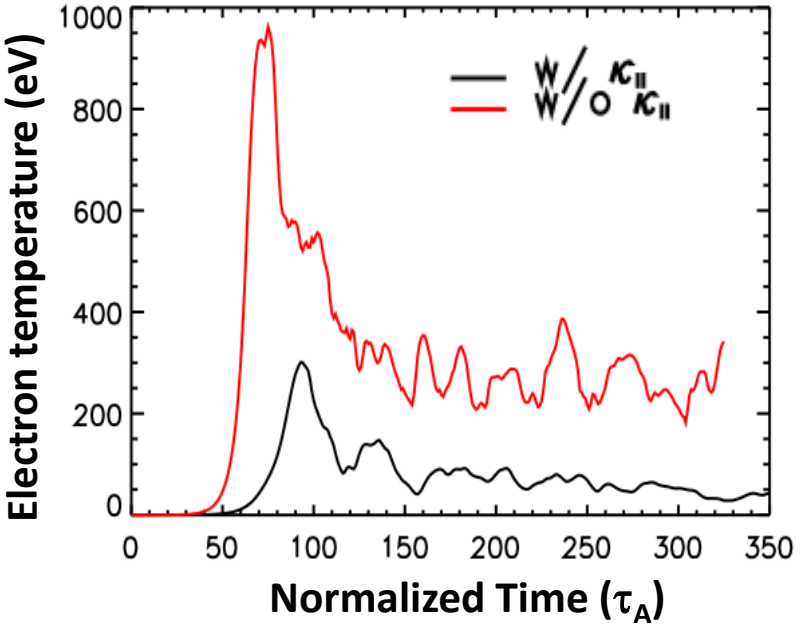

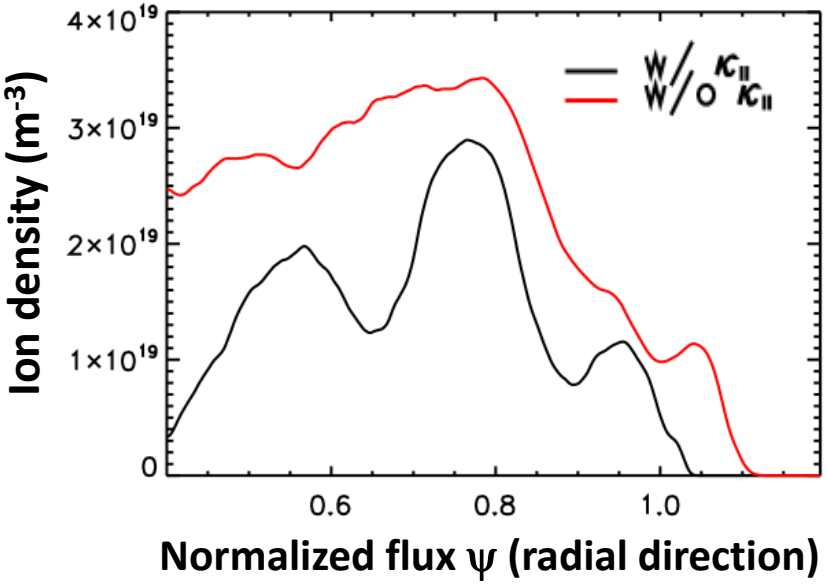

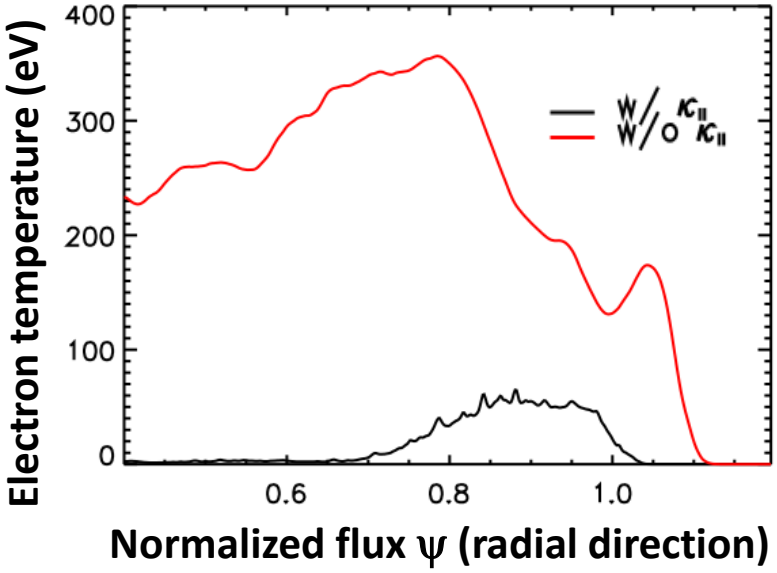

Convective particle transport is suppressed and narrowed by larger thermal conduction

With fixed pressure profile:

- Larger temperature ➔ larger $\kappa_{||j}$.
- Larger $\kappa_{||j}$ ➔ larger suppression effects .
- Larger suppression ➔ smaller and narrower radial convective transport.

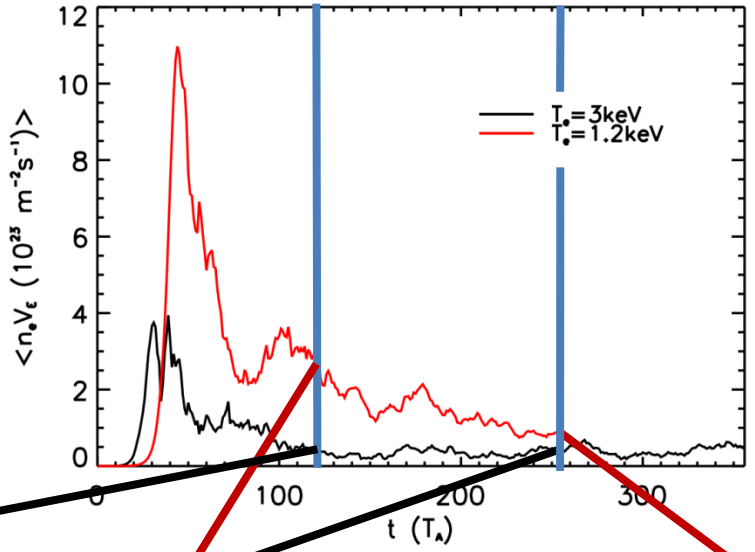

Radial particle transport (n_i * V_{Er} : $m^{-2}s^{-1}$):

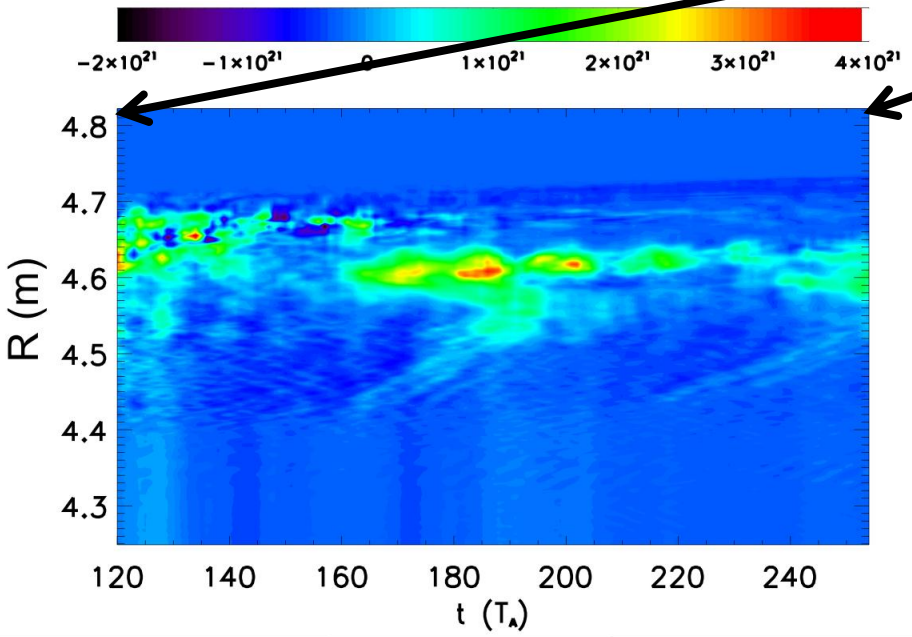

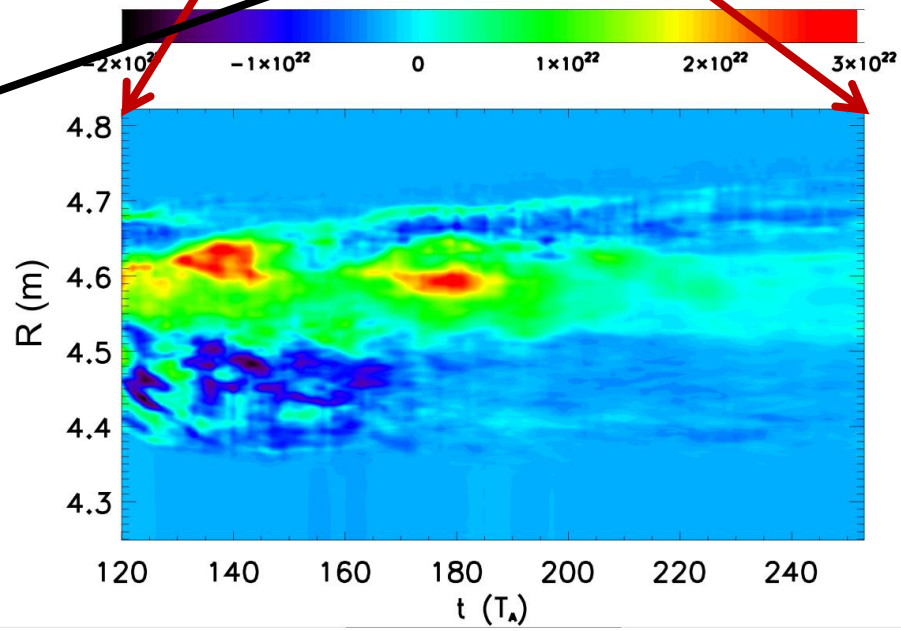

BOUT++ simulations show that the stripes from visible camera match ELM filamentary structures

EAST#41019@3034ms Visible camera shows bright ELM structure$

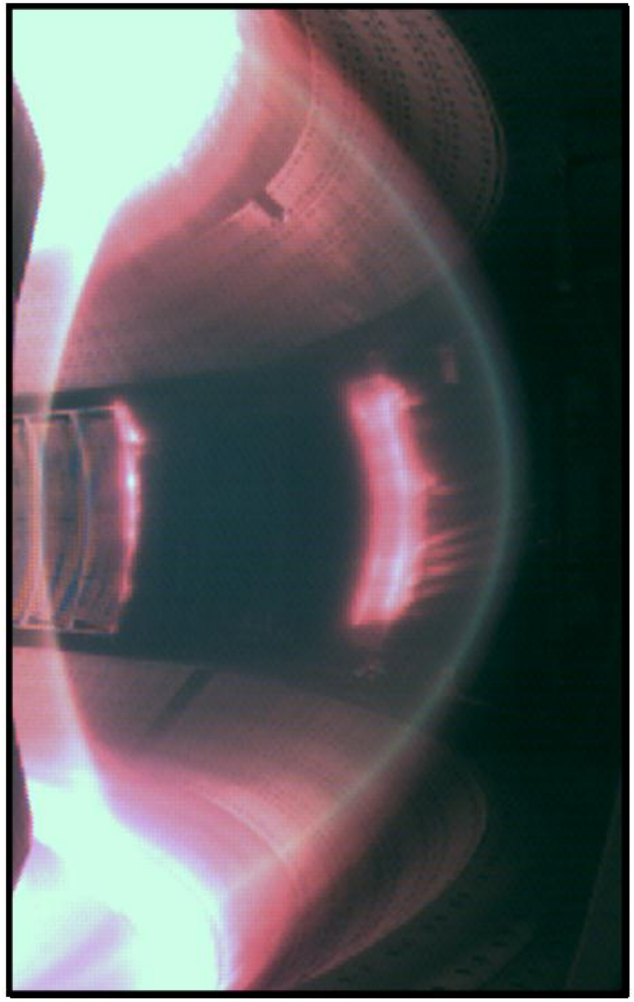

BOUT++ simulation shows that the ELM stripe are filamentary structures*

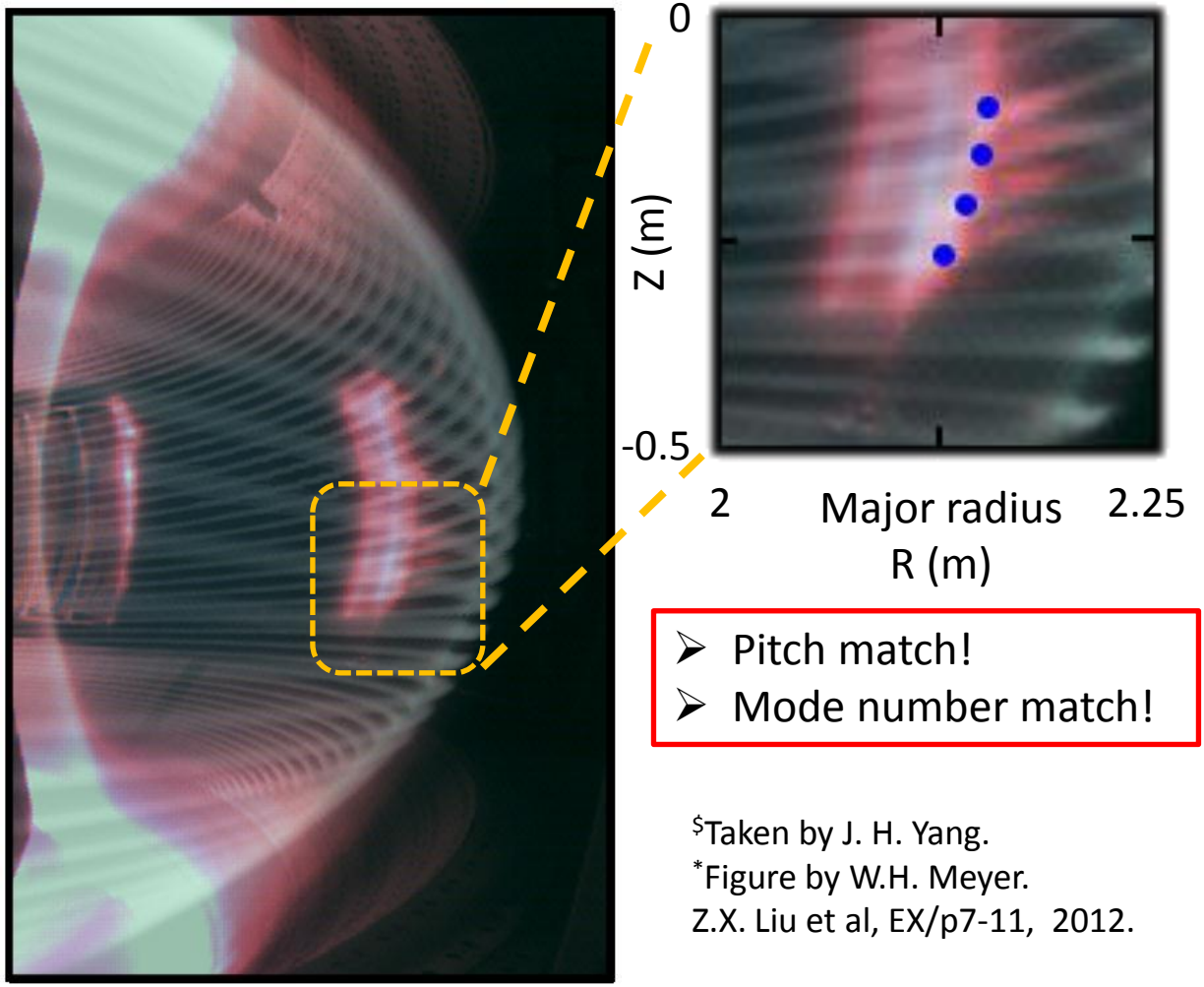

- Pitch match!
- Mode number match!

$Taken by J. H. Yang.
*Figure by W.H. Meyer.
Z.X. Liu et al, EX/p7-11, 2012.

Principal Results

(1) **Series of 2-fluid models are developed in BOUT++ to simulate ELM crash.**

(2) **Fundamental model: 3-field 2-fluid model is a good enough model for P-B stability and ELM crashes.**

(3) **6-field model is developed and it is well consistent with 3-field model. This model is a useful tool to study energy transport.**

(4) **High-n P-B mode is strongly stabilized at low density by diamagnetic drifts at low temperature.**

(5) **Thermal conductivities can sufficiently prevent the perturbations to penetrate into the inner boundary.**

(6) **Thermal conductivities can sufficiently suppress and narrow the particle transport at peak gradient region.**

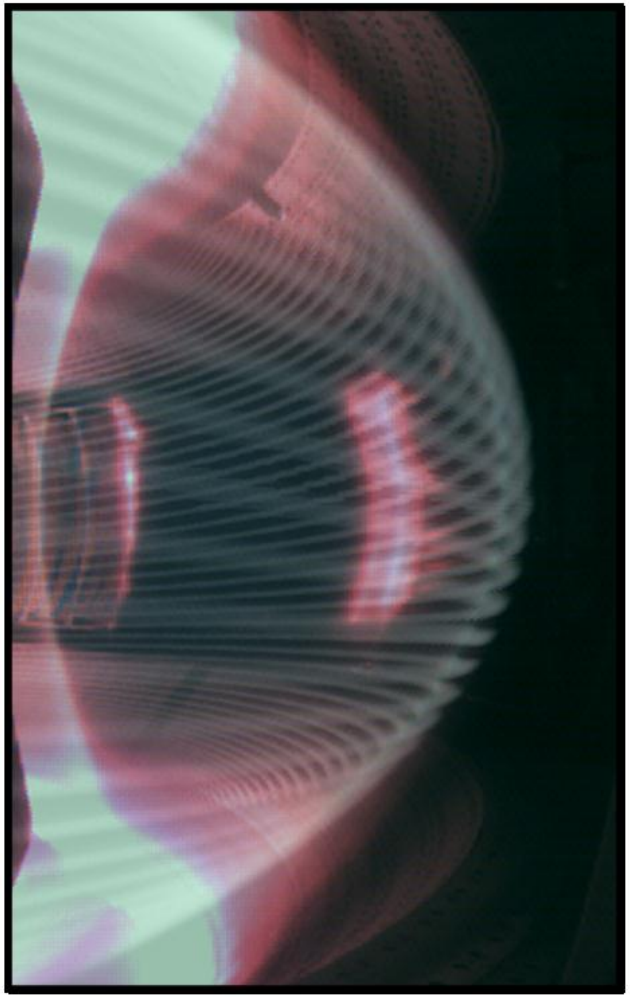

*Figure by Z. X. Liu, W.H. Meyer and J. H. Yang

ELM crash in BOUT++ simulations: linear growing

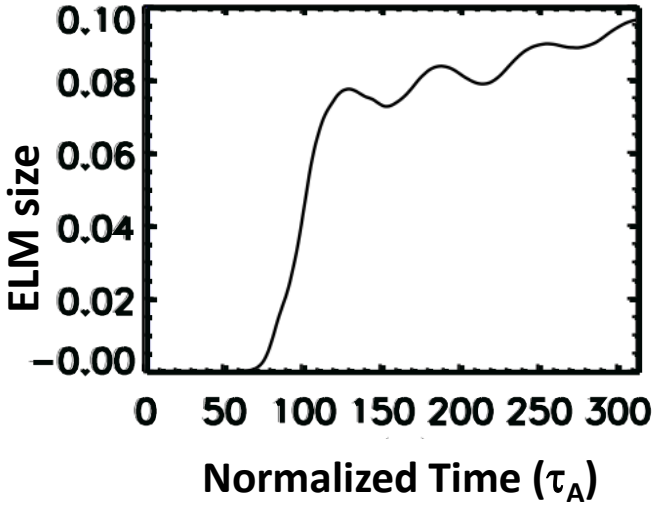

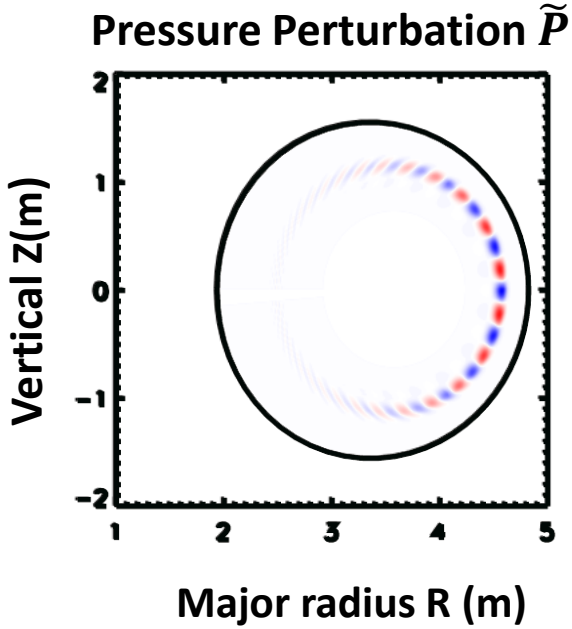

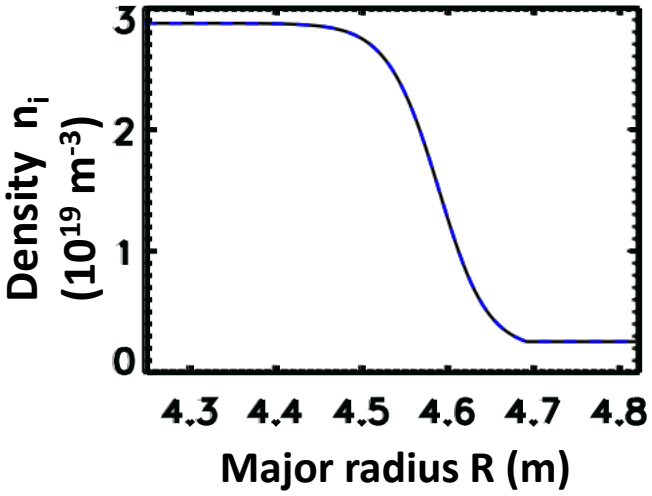

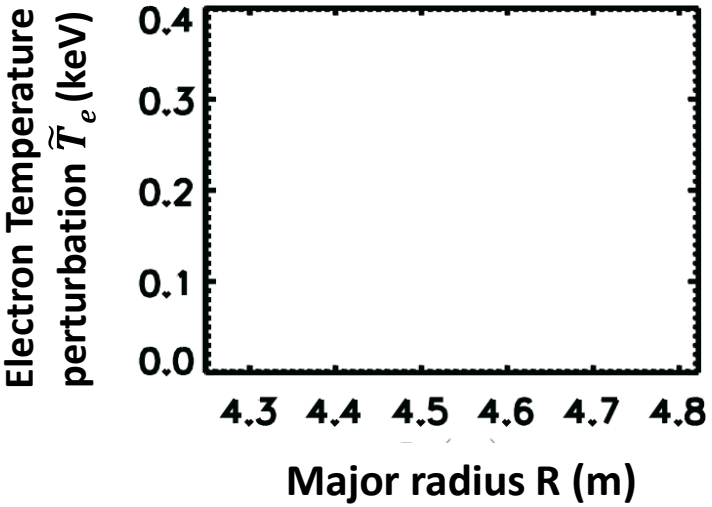

ELM crash in BOUT++ simulations

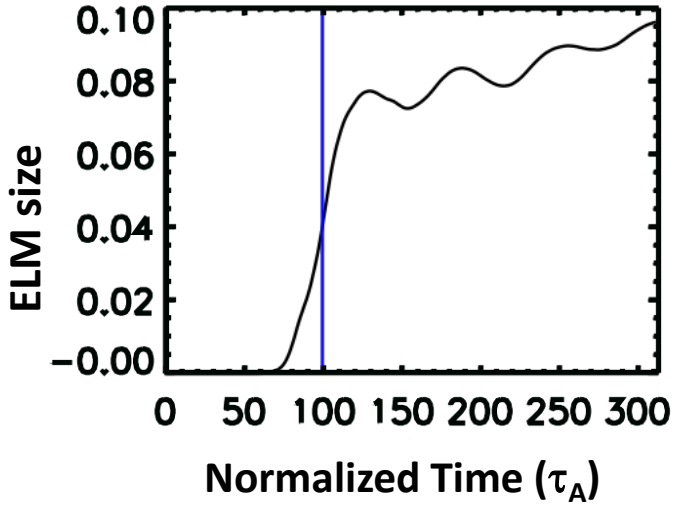

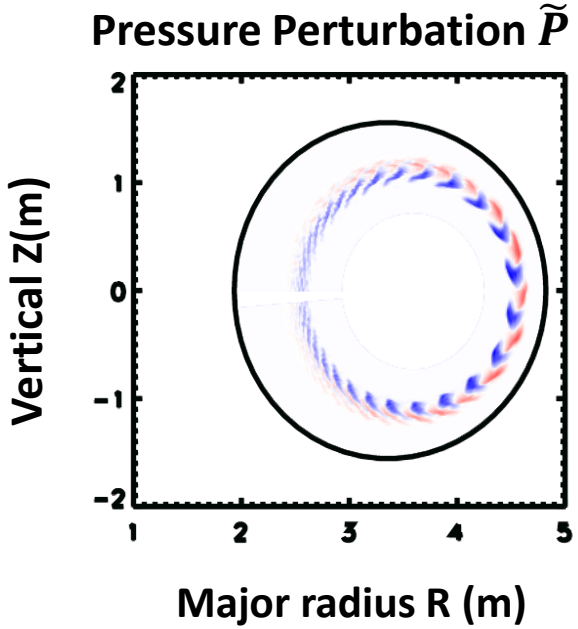

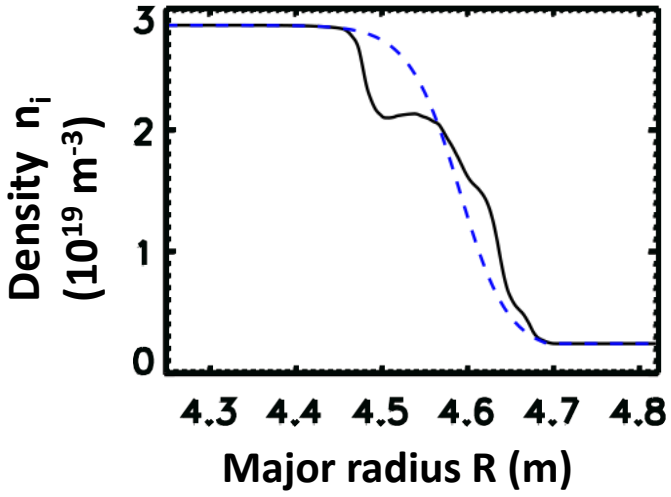

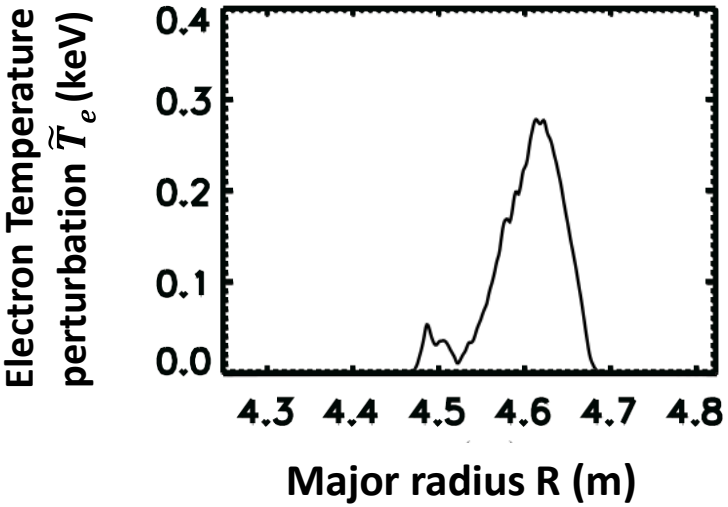

ELM crash in BOUT++ simulations

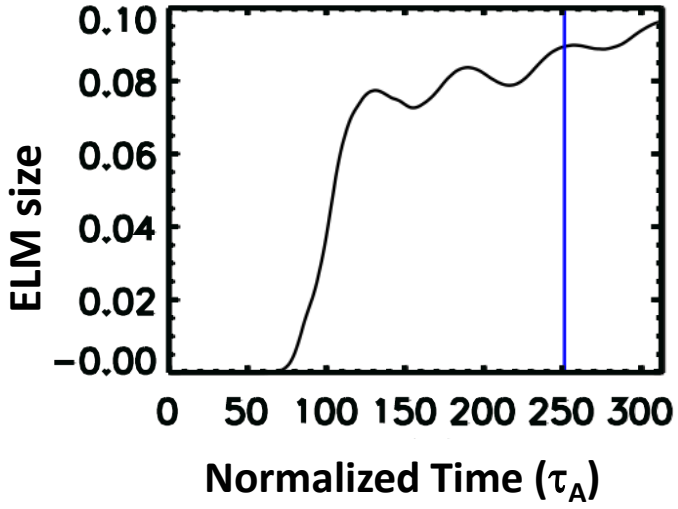

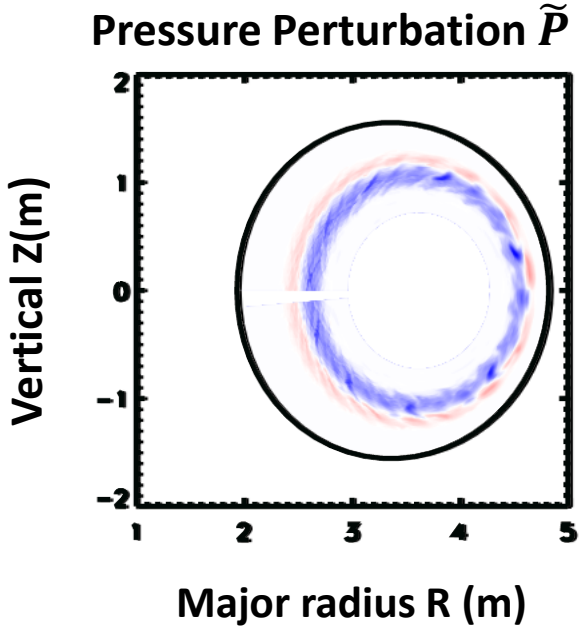

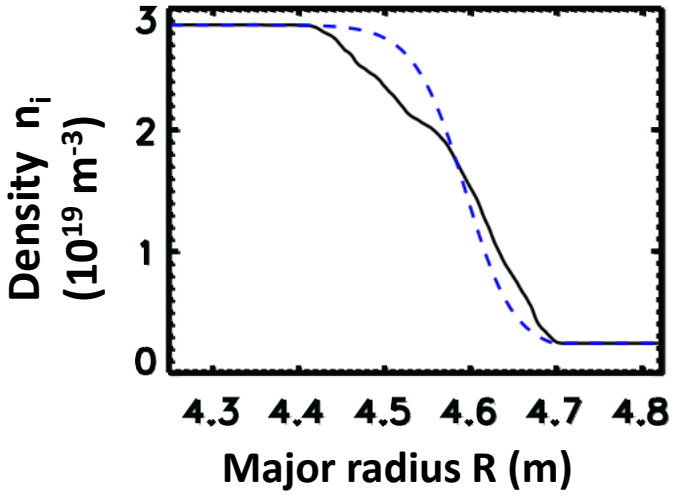

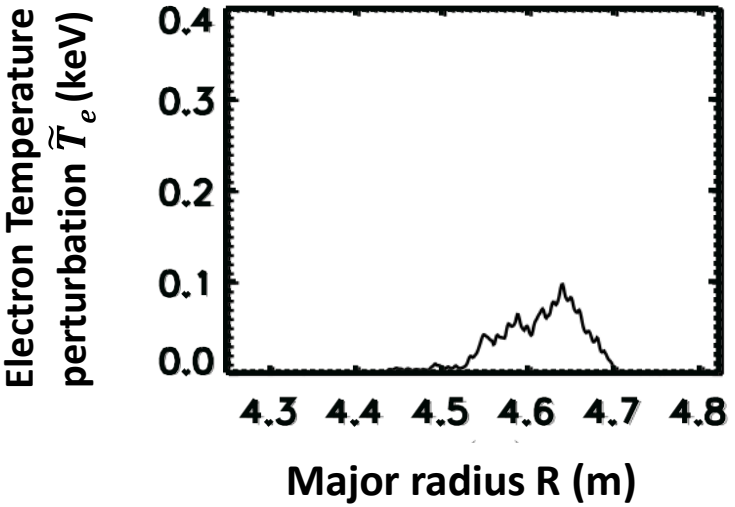

3-field 2-fluid model is good enough to simulate P-B stability and ELM crashes, additional physics from multi-field contributes less than 25% corrections

- **Fundamental physics in ELMs:**
  - ✓ Peeling-Ballooning instability
  - ✓ Ion diamagnetic stabilization
    - → kinetic effect
  - ✓ Resistivity and hyper-resistivity
    - → reconnection

- **Additional physics:**
  - Ion acoustic waves
  - Thermal conductivities
  - Hall effect
  - Compressibility
  - Electron-ion friction

change the linear growth rate less than 25%

Power depositions on PFCs. Turbulence and transport

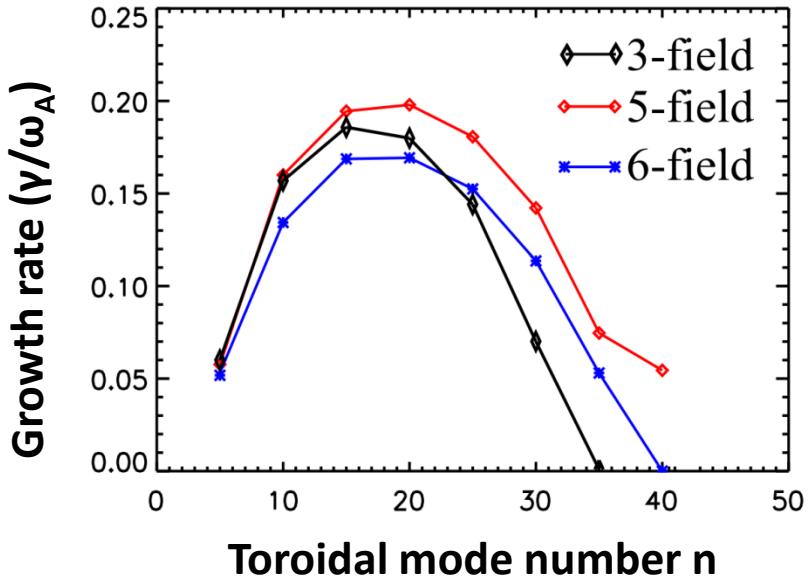

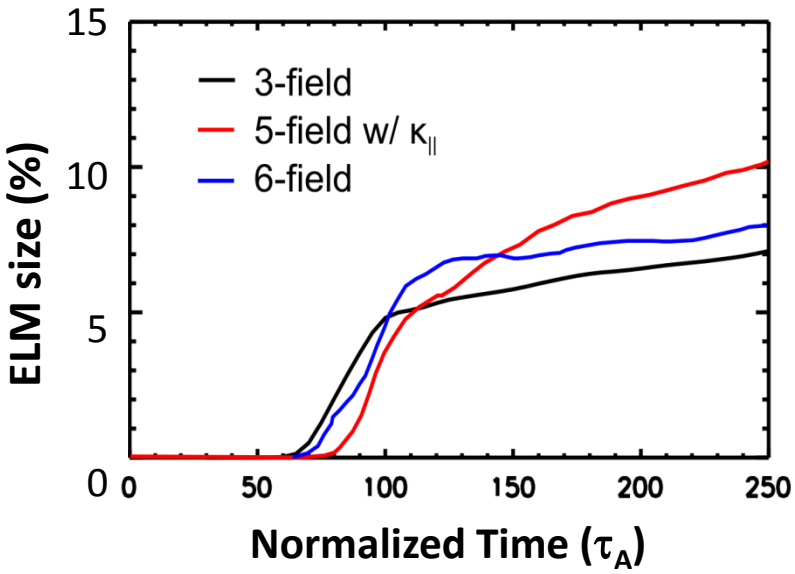

Thermal conductivities constrain the crash region

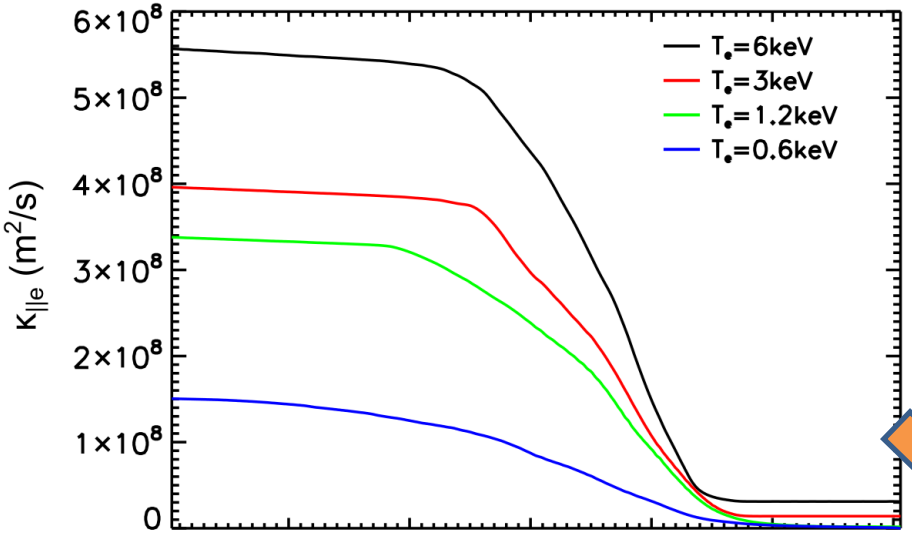

With fixed pressure profile:

- Larger $\kappa_{\|j}$ ➔ larger suppression effects on electric field.
- Smaller and narrower ExB drift ➔ narrower crash region.